Wave-equation common-angle gathers for converted waves

Paul Sava and Sergey Fomel, Bureau of Economic Geology, The University of Texas at Austin

SUMMARY

Seismic images obtained by multicomponent wave-equation migration can be decomposed into angle-gathers with a transformation that generalizes the equivalent construction for primary waves. A particularly simple formulation is to use all three components of the offset vector separating sources and receivers at image points. Using full vector offsets, multicomponent angle-gathers are built using simple transformations that are implemented partially in the Fourier domain and partially in the space domain.

INTRODUCTION

Downward wave extrapolation provides an accurate method for seismic imaging in structurally complex areas. Downward extrapolation methods have several known advantages in comparison with direct methods such as Kirchhoff migration due to their ability to handle multi-pathing, strong velocity heterogeneities, and finite-bandwidth wave-propagation effects (Gray et al., 2001).

In order to gain access to velocity and amplitude information, several authors (de Bruin et al., 1990; Prucha et al., 1999; Mosher and Foster, 2000; Rickett and Sava, 2002; Xie and Wu, 2002; Sava and Fomel, 2003; Soubaras, 2003; Biondi and Symes, 2004; Rosales and Biondi, 2005) suggested methods for constructing angle gathers from downward-continued wavefields. Those angle-gathers can be constructed either in the data space, prior to imaging, or in the image space, after imaging. These methods can be applied for shot-record and/or shot-geophone migration. The key element for imaging in the angle domain is the imaging condition, that must fulfill two requirements: it must preserve the velocity information during imaging, and it must allow angle decomposition after imaging.

Multicomponent imaging with converted waves gains increasing popularity, since converted waves sample complex geology differently from primary waves, thus giving us access to additional information about the media under investigation (Stewart et al., 2002, 2003). In particular, imaging multicomponent data in the angle domain leads to amplitude information (AVA) that can be accurately exploited by rock physics for rock and fluid properties that are different from those inferred from P waves.

Converted waves can be imaged with wavefield extrapolation, with a simple adaptation of the velocity used to extrapolate the various components of the data on the source and receiver sides. Converted waves imaging faces issues similar to those encountered by primary waves when analyzing image accuracy. We need to update the velocity models, but in order to do that we need to measure velocity inaccuracy. Thus, the challenge is to compute accurate angle gathers that give us access to velocity information.

This paper derives the angle decomposition for converted waves as a generalization of the analogous method for P waves. We present the theory of the method and illustrate it with examples highlighting its main features.

IMAGING CONDITION

A prestack imaging condition for wavefield extrapolation migration estimates reflectivity at every image point using the following expression (Sava and Fomel, 2005):

$$\mathbf{R}(\mathbf{m},\mathbf{h}) = \sum_{\omega} \mathbf{U}_s(\mathbf{m}-\mathbf{h},\omega)\,\overline{\mathbf{U}_r}(\mathbf{m}+\mathbf{h},\omega) \ . \tag{1}$$

Here, $\mathbf{m} = [m_x, m_y, m_z]$ is a vector describing the locations of image points, $\mathbf{h} = [h_x, h_y, h_z]$ is a vector describing the local source-receiver separation in the image space. m_x and m_y are the horizontal coordinates, and m_z is the depth coordinate of an image point relative to a reference coordinate system. The components of the $\mathbf{h}$ vector are the two conventional horizontal offsets, h_x and h_y (Rickett and Sava, 2002), and a vertical offset h_z (Biondi and Symes, 2004). The summation over temporal frequencies ω extracts the image $\mathbf{R}$ at zero time.

This imaging condition reveals data that are not mapped to zero-offset in the imaging process, indicating velocity inaccuracies and allowing angle-domain decompositions of the migrated images. $\mathbf{U}_s$ is the source wavefield extrapolated with the source slowness s_s, and $\mathbf{U}_r$ is the complex conjugate receiver wavefield extrapolated with the receiver slowness s_r. If the source and receiver wavefields correspond to P and S waves respectively, then the two slownesses can be written function of the P wave slowness $s(\mathbf{m})$ and the v_p/v_s ratio $\gamma(\mathbf{m})$ at every location in space: $s_s = s$ and $s_r = \gamma s$.

Reflectivity versus angle (RVA) analysis for converted waves requires image decomposition function of angles at every image point

$$\mathbf{R}(\mathbf{m},\mathbf{h}) \Longrightarrow \mathbf{R}(\mathbf{m},\theta_s,\theta_r) \ , \tag{2}$$

where θ_s is the angle made by the incident (source) ray with the normal to the reflector, and θ_r is the angle made by the reflected (receiver) ray with the normal to the reflector (Figure 1).

ANGLE DECOMPOSITION

Using the definitions introduced in the preceding section, we can make the standard notations for the source and receiver coordinates: $\mathbf{s} = \mathbf{m}-\mathbf{h}, \mathbf{r} = \mathbf{m}+\mathbf{h}$ The traveltime from a source to a receiver is a function of all spatial coordinates of the seismic experiment $t = t(\mathbf{m},\mathbf{h})$. Differentiating t with respect to all components of the vectors $\mathbf{m}$ and $\mathbf{h}$, and making the standard notations $\mathbf{p}_\alpha = \nabla_\alpha t$, where $\alpha = \{\mathbf{m},\mathbf{h},\mathbf{s},\mathbf{r}\}$, we can write:

$$\mathbf{p_m} = \mathbf{p_r} + \mathbf{p_s} \ , \tag{3}$$
$$\mathbf{p_h} = \mathbf{p_r} - \mathbf{p_s} \ . \tag{4}$$

By definition, $|\mathbf{p_s}| = s_s$ and $|\mathbf{p_r}| = s_r$, where s_s and s_r are slownesses associated with the source and receiver rays, respectively.

For computational reasons, it is convenient to define the angles θ and δ using the following relations:

$$2\theta = \theta_s + \theta_r \ , \ 2\delta = \theta_s - \theta_r \ . \tag{5}$$

Those two angles are the analogs of the image midpoint and offset coordinates. With these two angles, we can find the reflection angles θ_s and θ_r using the relations

$$\theta_s = \theta - \delta \ , \ \theta_r = \theta + \delta \ . \tag{6}$$

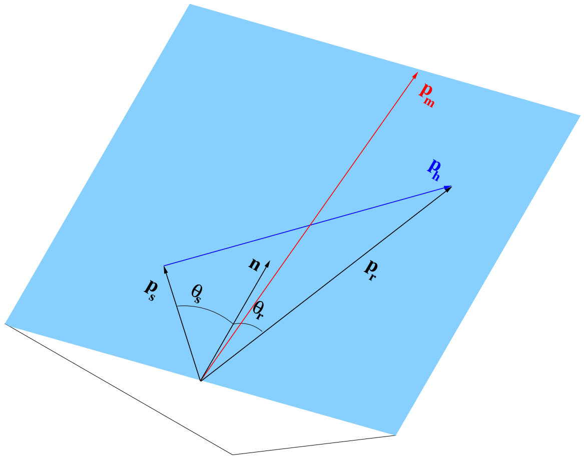

Figure 1: Geometric relations between ray vectors at a reflection point.

Angle 2θ represents the opening between and incident and a reflected ray, and angle δ represents the deviation of the bisector of the angle 2θ from the normal to the reflector. For P-P reflections, $\delta = 0$.

Reflection angle θ
By analyzing the geometric relations of various $\mathbf{p}_\alpha$ vectors (Figure 1), we can write the following trigonometric expressions:

$$|\mathbf{p_h}|^2 = |\mathbf{p_s}|^2 + |\mathbf{p_r}|^2 - 2|\mathbf{p_s}||\mathbf{p_r}|\cos(2\theta) , \quad (7)$$

$$|\mathbf{p_m}|^2 = |\mathbf{p_s}|^2 + |\mathbf{p_r}|^2 + 2|\mathbf{p_s}||\mathbf{p_r}|\cos(2\theta) , \quad (8)$$

$$\mathbf{p_m} \cdot \mathbf{p_h} = |\mathbf{p_r}|^2 - |\mathbf{p_s}|^2 . \quad (9)$$

We can transform this expression further using the notations $|\mathbf{p_s}| = s$ and $|\mathbf{p_r}| = \gamma s$, where $\gamma(\mathbf{m})$ is the v_p/v_s ratio, and $s(\mathbf{m})$ is the slowness associated with the incoming ray at every image point.

Solving for $\tan\theta$ from equations (7) and (8), we obtain an expression for the reflection angle function of position and offset wavenumbers $(\mathbf{k_m}, \mathbf{k_h})$:

$$\boxed{\tan^2\theta = \frac{(1+\gamma)^2|\mathbf{k_h}|^2 - (1-\gamma)^2|\mathbf{k_m}|^2}{(1+\gamma)^2|\mathbf{k_m}|^2 - (1-\gamma)^2|\mathbf{k_h}|^2} .} \quad (10)$$

For the particular case of incident and reflected P waves ($\gamma = 1$), equation (10) takes the form (Sava and Fomel, 2005)

$$\tan\theta_0 = \frac{|\mathbf{k_h}|}{|\mathbf{k_m}|} . \quad (11)$$

Using equations (10) and (11), we can write:

$$\tan^2\theta = \frac{(1+\gamma)^2\tan^2\theta_0 - (1-\gamma)^2}{(1+\gamma)^2 - (1-\gamma)^2\tan^2\theta_0} . \quad (12)$$

Equation (12) can be used to compute converted-wave angle gathers as a succession of operations: first, we compute angle gathers using equation (11) in the Fourier domain, and then we correct those gathers in the space domain by a stretch that depends on the local v_p/v_s ratio $\gamma(\mathbf{m})$.

Reflection angle δ
According to Snell's law, we can write at every image point

$$\frac{\sin\theta_s}{\sin\theta_r} = \frac{|\mathbf{p_r}|}{|\mathbf{p_s}|} = \gamma(\mathbf{m}) . \quad (13)$$

Using the definitions of the angles made by the incident and reflected rays with the normal to the reflector at the reflection point, equations (6), we can write the following trigonometric identity:

$$\frac{\sin(\theta+\delta)}{\sin(\theta-\delta)} = \frac{\tan\theta - \tan\delta}{\tan\theta + \tan\delta} . \quad (14)$$

After simple algebraic manipulations, we obtain an expression that allows us to compute at every image point the angle δ function of the angle θ and the local v_p/v_s ratio.

$$\boxed{\tan\delta = \frac{1-\gamma}{1+\gamma}\tan\theta .} \quad (15)$$

For the particular case of P-P reflections ($\gamma = 1$), equation (15) takes the form

$$\tan\delta_0 = 0 , \quad (16)$$

indicating that for P waves, the incident and reflected angles are symmetric relative to the reflector normal.

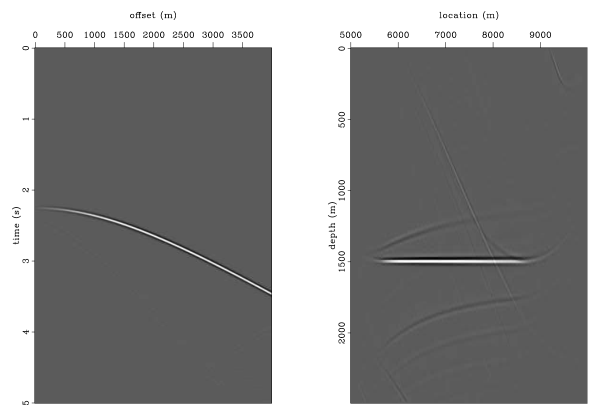

Figure 2: Synthetic data (left) and migrated image (right).

OTHER FORMULATIONS

The system (7)-(9) provides an implicit dependency of the reflection angle θ on the local slowness s and the three-dimensional coordinates of the position and offset ray parameter vectors, $\mathbf{p_m}$ and $\mathbf{p_h}$, respectively. In principle, we can eliminate any 2 parameters from this system to get an expression for the reflection angle. For example, if we eliminate the slowness s and the product $\mathbf{p_m} \cdot \mathbf{p_h}$, we obtain the expression (10).

Alternatively, we can eliminate other pairs of variables and obtain angle mapping equations that fulfill various acquisition or processing requirements. However, none of these expressions is as compact as equation (10). For example, we can eliminate the vertical offset k_{h_z} and the local slowness s. This is the case when we want to avoid computing explicitly the vertical offset h_z during imaging. For a 2-D reflector, the expression for the reflection angle is:

$$\tan\theta = \frac{(1+\gamma)(a_{hx}+b_{mx})}{2\gamma k_{m_z} + \sqrt{4\gamma^2 k_{m_z}^2 + (\gamma^2-1)(a_{hx}+b_{mx})(a_{mx}+b_{hx})}} , \quad (17)$$

where we use the notations $a_{hx} = (1+\gamma)\,k_{h_x}$, $a_{mx} = (1+\gamma)\,k_{m_x}$, $b_{hx} = (1-\gamma)\,k_{h_x}$, and $b_{mx} = (1-\gamma)\,k_{m_x}$. For a flat reflector ($k_{m_x} = 0$), this expression reduces to

$$\tan\theta = \frac{(1+\gamma)^2 k_{h_x}}{2\gamma k_{m_z} + \sqrt{4\gamma^2 k_{m_z}^2 - (\gamma^2-1)^2 k_{h_x}^2}} . \quad (18)$$

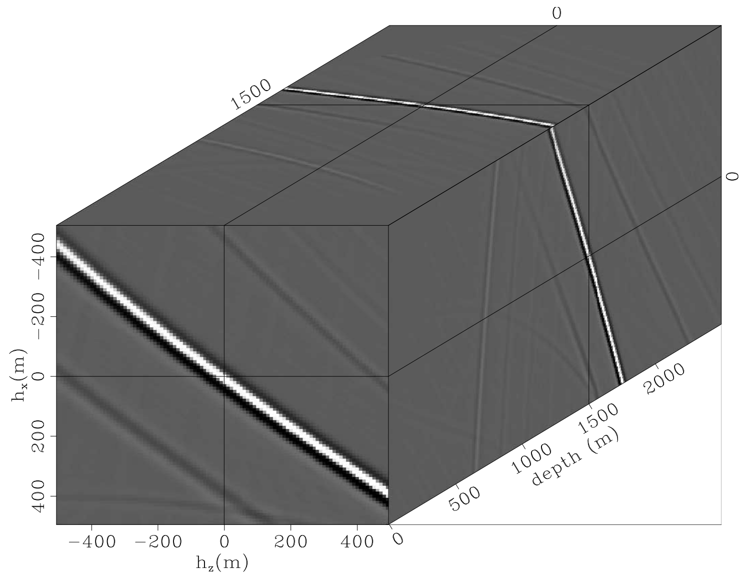

Figure 3: Multi-offset converted-waves common-image gather. The vertical offset $h_z \neq 0$ even for flat reflectors.

In the case of P-P reflections ($\gamma = 1$), equation (18) reduces to the known expression (Sava and Fomel, 2003)

$$\tan\theta = \frac{k_{h_x}}{k_{m_z}} . \tag{19}$$

Another particular solution of the system (7)-(9) can be achieved by eliminating the depth and the vertical offset wavenumbers, k_{m_z} and k_{h_z}. This situation corresponds to the case in which we want to compute angle decompositions in the data space, prior to imaging. In this situation, the system (7)-(9) can be solved for an implicit relation of the reflection angle θ with other spatial quantities. For a 2-D reflector, this expression is

$$\begin{aligned}(a_{mx}+b_{hx})\tan^4\theta + 4b_{mx}a_{hx}\tan^2\theta\,(a_{hx}+b_{mx}) = \\ 2\tan^2\theta\left[8\gamma^2 s^2\omega^2 - \left(1+\gamma^2\right)k_{m_x}^2 - \left(1+\gamma^2\right)k_{h_x}^2\right] .\end{aligned} \tag{20}$$

In the case of $\gamma = 1$, equation (20) reduces to the form derived by Fomel (2004).

Another possibility is to eliminate the dip dependence from the system (7)-(9). In 2-D, we obtain the dip-independent relation

$$\left(\gamma^2-1\right)\left(k_{m_z}-k_{h_z}\right) + 2\left(\gamma+1\right)k_{m_z}\sin^2\theta = 4k_{h_x}\gamma\cos\theta\sin\theta . \tag{21}$$

The bottom line is that formulation (7)-(9) provides, in principle, the theoretical framework for many different implementations of angle decomposition, both prior and after imaging. However, neither form is as simple and compact as equations (10) and (15).

This solution requires computation of the third component of the offset vector, which is not normally done in wave-equation imaging. However, a careful implementation of shot-record migration gives us a fairly simple option to compute this quantity. In particular, we can avoid computing the vertical offset h_z, as well as the horizontal offsets h_x and h_y, at locations that are not of interest for either velocity analysis or AVA analysis. For example, we can select sparse positions in space and/or sparse horizons, and avoid computing the costly cross-correlations at other locations. This procedure, used in this paper, considerably speeds-up the imaging condition for shot-record migration. Furthermore, since equation (10) depends only on the absolute magnitude of the offset wavenumber $|\mathbf{k_h}| = k_{|\mathbf{h}|}$, we can store only the magnitude of the offset vector during the imaging cross-correlation, thus saving memory and disk space, particularly in 3-D.

IMPLEMENTATION

Equations (10) and (15) depend both on Fourier domain quantities, $\mathbf{k_m}$ and $\mathbf{k_h}$, and on space domain quantities, $\gamma(\mathbf{m})$. This transformation can be implemented in a sequence of two transformations. In the first transformation, we can convert $\mathbf{R}(\mathbf{m},\mathbf{h})$ to $\mathbf{R}(\mathbf{m},\theta_0)$ in the Fourier domain, using equation (11). Then we can transform $\mathbf{R}(\mathbf{m},\theta_0)$ to $\mathbf{R}(\mathbf{m},\theta,\delta)$ in the space domain using equations (12) and (15).

The algorithm for converting multi-offset reflectivity into multi-angle reflectivity is the following:

	$\mathbf{U}_s(\omega,\mathbf{m}+\mathbf{h}),\overline{\mathbf{U}_r}(\omega,\mathbf{m}-\mathbf{h})$
Imaging (1)	$\Downarrow$
	$\mathbf{R}(\mathbf{m},\mathbf{h})$
FFT (**m** & **h**)	$\Downarrow$
	$\mathbf{R}(\mathbf{k_m},\mathbf{k_h})$
K-domain mapping (11)	$\Downarrow$
	$\mathbf{R}(\mathbf{k_m},\tan\theta_0)$
IFT (**m**)	$\Downarrow$
	$\mathbf{R}(\mathbf{m},\tan\theta_0)$
X-domain mapping (12) and (15)	$\Downarrow$
	$\mathbf{R}(\mathbf{m},\tan\theta,\tan\delta)$

EXAMPLE

We illustrate the multicomponent angle-gather construction with a simple model of a flat reflector in constant velocity. The left panel of figure 2 shows one typical shot gather, and the right panel shows the image obtained by shot-record migration. The shot is located at 5500 m and the flat reflector is at 1500 m depth. The incident P-wave velocity is 2000 m/s and the reflected S-wave velocity is 1000 m/s. Given the geometry of our simple experiment, Figure 4, the incident P wave arrives at the image location at 45°, and the reflected S wave leaves the image point at approximately 21° from the normal.

Figure 3 shows one common-image gather at 4000 m. The from panel of the cube depicts the horizontal and vertical offsets, h_x and h_z respectively. For a P-P reflection, the offset vector is parallel to the reflector (horizontal in this case), therefore its vertical component $h_z = const$. This is not true for P-S reflections, even for this simple case of a flat

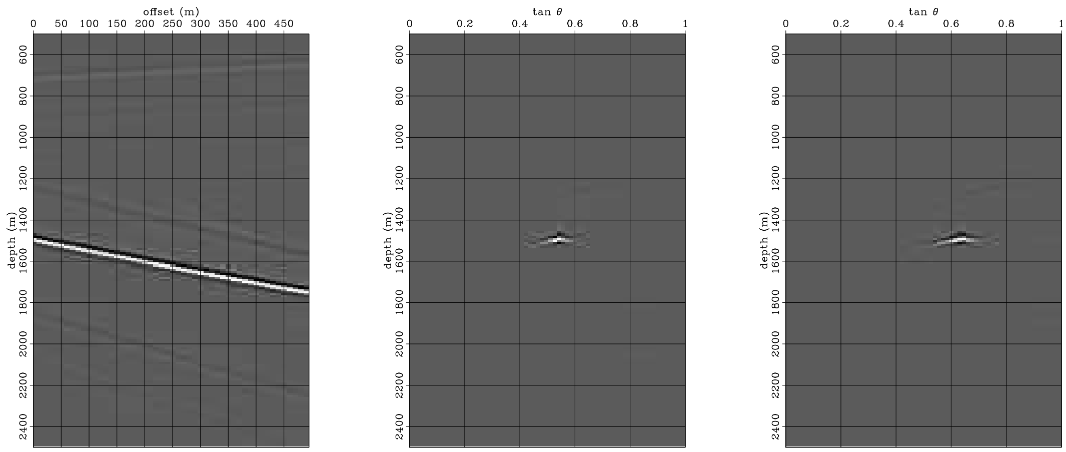

Figure 5: Offset-gather for a single shot (left), angle-gather constructed using the traditional P-P methodology, and angle-gather constructed using the converted methodology.

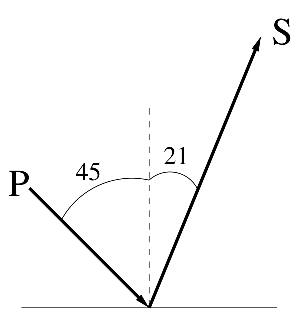

Figure 4: Simple converted-wave reflection experiment.

reflector in constant media. Figure 3 illustrates that both offsets are non-zero, which invalidates the conventional common-angle constructions that are designed for P-P reflections.

Figure 5 (middle panel) shows that conventional angle-domain mapping misplaces the reflected energy: the reflection is placed at $\tan\theta \approx 0.55$ corresponding to an incorrect reflection angle of $2\theta \approx 57^\circ$. Figure 5 (right panel) shows the same angle-gather after converted wave correction. Now, the energy is correctly places at $\tan\theta \approx 0.65$ which corresponds to a correct reflection angle $2\theta \approx 66^\circ$.

CONCLUSION

We implement angle decomposition for images constructed with shot-record migration of multicomponent data. We use full vector offsets separating sources and receivers at image points. This approach leads to a compact formulation for the incidence and reflection angles at every image points. A simple numerical experiment confirms the theory.

REFERENCES

Biondi, B., and Symes, W. W., 2004, Angle-domain common-image gathers for migration velocity analysis by wavefield-continuation imaging: Geophysics, **69**, 1283–1298.

de Bruin, C. G. M., Wapenaar, C. P. A., and Berkhout, A. J., 1990, Angle-dependent reflectivity by means of prestack migration: Geophysics, **55**, 1223–1234.

Fomel, S., 2004, Theory of 3-D angle gathers in wave-equation imaging *in* 74th Ann. Internat. Mtg. Soc. of Expl. Geophys.

Gray, S. H., Etgen, J., Dellinger, J., and Whitmore, D., 2001, Seismic migration problems and solutions: Geophysics, **66**, 1622–1640.

Mosher, C., and Foster, D., 2000, Common angle imaging conditions for prestack depth migration *in* 70th Ann. Internat. Mtg. Soc. of Expl. Geophys., 830–833.

Prucha, M., Biondi, B., and Symes, W., 1999, Angle-domain common image gathers by wave-equation migration *in* 69th Ann. Internat. Mtg. Soc. of Expl. Geophys., 824–827.

Rickett, J. E., and Sava, P. C., 2002, Offset and angle-domain common image-point gathers for shot-profile migration: Geophysics, **67**, 883–889.

Rosales, D., and Biondi, B., 2005, Converted-wave angle-domain common-image gathers. *in* 75th Ann. Internat. Mtg. Soc. of Expl. Geophys.

Sava, P., and Fomel, S., 2005, Coordinate-independent angle-gathers for wave equation migration *in* 75th Ann. Internat. Mtg. Soc. of Expl. Geophys.

Sava, P. C., and Fomel, S., 2003, Angle-domain common-image gathers by wavefield continuation methods: Geophysics, **68**, 1065–1074.

Soubaras, R., 2003, Angle gathers for shot-record migration by local harmonic decomposition *in* 73rd Ann. Internat. Mtg. Soc. of Expl. Geophys., 889–892.

Stewart, R. R., Gaiser, J., Brown, R. J., and Lawton, D. C., 2002, Converted-wave seismic exploration: Methods: Geophysics, **67**, 1348–1363.

—, 2003, Converted-wave seismic exploration: Applications: Geophysics, **68**, 40–57.

Xie, X., and Wu, R., 2002, Extracting angle domain information from migrated wavefield *in* 72nd Ann. Internat. Mtg. Soc. of Expl. Geophys., 1360–1363.